Rhizosphere 38 (2026) 101335

Contents lists available at ScienceDirect

Rhizosphere

journal homepage: www.elsevier.com/locate/rhisph

A new *Priestia aryabhattai* isolate suppresses chili pepper southern blight: Field and laboratory evidence for broad-spectrum antifungal activity

Wanida Petlamul [a], Sawai Boukaew [a,*], Sudarat Chumjan [a], Natthawut Chuaikaeo [a], Premmika Tengchiang [a], Benjamas Cheirsilp [b], Siriporn Yossan [c], Sirasit Srinuanpan [d], Krittin Chumkaew [e]

[a] Faculty of Agricultural Technology, Songkhla Rajabhat University, Songkhla, 90000, Thailand
[b] Center of Excellence in Innovative Biotechnology for Sustainable Utilization of Bioresources, Faculty of Agro-Industry, Prince of Songkla University, Hatyai, 90110, Thailand
[c] Division of Environmental Science, Faculty of Liberal Arts and Science, Sisaket Rajabhat University, Sisaket, 33000, Thailand
[d] Center of Excellence in Microbial Diversity and Sustainable Utilization, Chiang Mai University, Chiang Mai, 50200, Thailand
[e] Department of Food and Nutrition, Faculty of Home Economics Technology, Rajamangala University of Technology Thanyaburi, Pathum Thani, 12110, Thailand

ARTICLE INFO

Keywords:
Biological control
Antifungal metabolites
Plant–microbe interactions
Rhizobacteria
Disease suppression

ABSTRACT

Sclerotium rolfsii, the causal agent of southern blight, causes significant yield losses in chili pepper. Beneficial rhizosphere bacteria represent promising alternatives for sustainable disease management. In this study, thirteen bacterial isolates from the chili pepper rhizosphere were screened for antifungal activity, and a highly effective isolate was selected for further investigation. Whole-genome sequencing identified the isolate as *Priestia aryabhattai*, and antiSMASH analysis combined with LC–QTOF–MS profiling revealed multiple putatively identified metabolites, including cyclic peptides, lipid-related compounds, and previously reported bioactive molecules. Culture filtrates (CF) strongly inhibited mycelial growth (up to 99.8%) and completely suppressed sclerotia formation, while exhibiting broad-spectrum antifungal activity against ten phytopathogenic fungi. Application of the isolate enhanced chili seed germination and early seedling growth. In greenhouse trials, bacterial treatment improved seedling survival, showing efficacy comparable to fungicide treatment under the conditions tested. Field trials further demonstrated a substantial reduction in disease severity (73%), supporting effective pathogen mitigation across multiple experimental systems. Mechanistic investigations revealed mycolytic activity and disruption of redox homeostasis in *S. rolfsii*, as evidenced by increased ROS accumulation and altered antioxidant enzyme activities. Collectively, these findings support effective pathogen mitigation linked to mechanistic insights, highlighting *P. aryabhattai* R-KT-26 as a promising candidate for sustainable biological control of chili pepper southern blight.

1. Introduction

Chili pepper (*Capsicum annuum* L.) is an economically important vegetable crop cultivated worldwide, including Thailand, and is frequently affected by soil-borne pathogens. Among these, southern blight caused by *Sclerotium rolfsii* is a highly destructive disease, as the pathogen can survive in soil through resilient sclerotia and infect a wide range of host plants (Javaid et al., 2023; Qiu et al., 2024). Infection results in wilting, root and stem rot, and stunted growth, ultimately leading to significant yield losses (Ali et al., 2020; Jia et al., 2026).

Management of *S. rolfsii* remains challenging due to its persistence in soil and broad host range (Jia et al., 2026). Chemical fungicides are commonly used; however, intensive application can result in environmental contamination and the emergence of resistant pathogen populations (Li et al., 2021; Ceresini et al., 2024). These limitations highlight the need for sustainable alternatives that can provide effective and reliable pathogen mitigation under practical cultivation conditions.

Rhizosphere bacteria, particularly *Bacillus* spp., have demonstrated effective suppression of *S. rolfsii* through multiple mechanisms, including the production of antifungal metabolites (e.g., lipopeptides and polyketides), secretion of hydrolytic enzymes that degrade fungal cell walls, emission of inhibitory volatile compounds, and competitive

* Corresponding author.
E-mail address: sawai.bo@skru.ac.th (S. Boukaew).

https://doi.org/10.1016/j.rhisph.2026.101335
Received 8 January 2026; Received in revised form 7 April 2026; Accepted 8 April 2026
Available online 11 April 2026

colonization of the rhizosphere (Jia et al., 2023; Li et al., 2023; Moon and Sang, 2024; Qiu et al., 2024). Genomic analyses of related *Priestia aryabhattai* strains have identified biosynthetic gene clusters and genes associated with plant growth promotion, providing molecular evidence of potential biocontrol activity (Pal et al., 2025). Other rhizosphere-associated genera, including *Pseudomonas*, *Trichoderma*, *Burkholderia*, and *Streptomyces*, have also been reported to suppress fungal pathogens through comparable mechanisms (García-Montelongo et al., 2023; Meena et al., 2024).

Despite these advances, many studies remain limited to *in vitro* assays or provide only partial mechanistic insights, with relatively few demonstrating consistent pathogen mitigation across laboratory, greenhouse, and field conditions. Furthermore, studies integrating genomic analysis, metabolite profiling, and mechanistic validation with field-level efficacy are still scarce. Such comprehensive approaches are essential for identifying biocontrol agents capable of stable performance under real agricultural conditions.

In this study, we aimed to (i) isolate and identify rhizosphere bacteria with antagonistic activity against *S. rolfsii*, (ii) characterize their antifungal mechanisms and bioactive metabolites, and (iii) evaluate the biocontrol potential of *P. aryabhattai* R-KT-26 under both greenhouse and field conditions. This study provides an integrated assessment of pathogen mitigation supported by mechanistic insights, highlighting the potential application of this strain in sustainable disease management.

2. Material and methods

2.1. Source of materials

2.1.1. Chili pepper

Chili pepper seeds (*Capsicum annuum* L. cv. 'Super Hot 2 F1') were used in this study. Prior to each experiment, seeds were surface-sterilized by soaking in 1% sodium hypochlorite (NaOCl) for 2 min, followed by rinsing three times with sterile distilled water for 1 min each.

2.1.2. Plant pathogenic fungi and culture conditions

The fungal pathogen *S. rolfsii* Sacc. isolate KKU 01 used in this study was obtained from the Mycorrhiza and Mycotechnology Laboratory, Department of Microbiology, Faculty of Science, Khon Kaen University, Thailand. The isolate was routinely cultured on potato dextrose agar (PDA; Himedia®, India) and incubated at 28 ± 2 °C for 3 days to promote active mycelial growth. To stimulate sclerotia formation, the culture was further incubated for 10 days before being used in subsequent experiments.

For inoculum preparation, a 5-mm mycelial plug from a 3-day-old *S. rolfsii* culture was transferred into sterile wheat seeds and incubated at 28 ± 2 °C for 10 days. The colonized wheat seeds were thoroughly ground using a mechanical blender and stored at 4 °C until further use in the study.

Other phytopathogenic fungi, including *Schizophyllum commune* Fr. (SOPRC-07), *Lasiodiplodia theobromae* (Pat.) Griffon & Maubl. (NM-01), *Peniophora salaccae* Boukaew et al. (2024) (SKRU002), *Curvularia oryzae* Bugnicourt (SOPRC-9), *Aspergillus parasiticus* Speare (TISTR 3276), *Aspergillus flavus* Link (PSRDC-4), *Rhizoctonia solani* J.G. Kühn (PTRRC-9), and *Colletotrichum musae* (Berk. & M.A. Curtis) Arx (NYB-03), were sourced from the Plant Pathology Laboratory, Faculty of Agricultural Technology, Songkhla Rajabhat University, Thailand. Additional isolates of *Corynespora cassiicola* (Berk. & M.A. Curtis) C.T. Wei (PSU-01) and *Fusarium incarnatum* (Desm.) Sacc. (PSU-01) were kindly supplied by Prof. Dr. Anurag Sunpapao (Agricultural Innovation and Management Division, Faculty of Natural Resources, Prince of Songkla University, Thailand). All fungal cultures were preserved on PDA slants and stored at 4 °C until further use.

2.1.3. Synthetic fungicide

Three commercial fungicides were evaluated in this study: propiconazole (25% w/v), azoxystrobin (25% w/v), and prochloraz (45% w/v). These products are commonly used in agricultural practice and are available in Thailand. Stock formulations were diluted to obtain final concentrations of 0.1–0.8% (v/v), calculated based on their respective active ingredient (a.i.) contents.

2.2. Isolation of antagonistic rhizobacteria

Five chili pepper rhizosphere soil samples were collected from different sites in Ko Taeo Subdistrict (7.092140° N, 100.622502° E), Mueang Songkhla District, Songkhla Province, Thailand. One gram of each soil sample was suspended in 9 ml of sterile saline solution (0.85% NaCl) and shaken on a rotary shaker at 150 rpm at 28 ± 2 °C for 24 h. The resulting soil suspensions were serially diluted up to 10^{-7}, and 0.1 ml aliquots from the 10^{-5} to 10^{-7} dilutions were spread onto nutrient agar (NA; HiMedia™) plates and incubated at 37 °C. After 5 days, different single colonies were picked on a new NA for streak purification and culture, and the obtained pure strains were transferred into NA slant medium and stored at 4 °C.

2.3. Screening for antifungal activity

2.3.1. Dual culture assay

All bacterial isolates were evaluated for their antagonistic activity against *S. rolfsii* using the dual culture technique (Mannaa et al., 2025). A loopful of each isolate was inoculated into 5 ml of nutrient broth (NB; HiMedia™) and incubated on a rotary shaker at 150 rpm and 37 °C for 24 h. Subsequently, a loopful of the 24 h-old culture (approximately 10^7 CFU/ml) was streaked onto one side of a NA plate and incubated under the same conditions for another 24 h to allow bacterial growth. After incubation, a 5 mm diameter mycelial plug taken from a 3-day-old *S. rolfsii* colony was placed on the opposite side of the plate, approximately 5 cm away from the bacterial streak. For the control, a mycelial plug of *S. rolfsii* was placed on an uninoculated NA plate. All plates were incubated at 28 ± 2 °C for 3 days. The radial growth of *S. rolfsii* toward the bacterial colony (treatment) and in the control was measured. The percentage inhibition was calculated using the following formula: inhibition (%) = $[(D_1 - D_2)/D_1] \times 100$, where D_1 is the radial growth of *S. rolfsii* in the control plate, and D_2 is the radial growth in the presence of bacterial isolates. Each experiment was performed twice with triplicate in each trial.

2.3.2. Volatile organic compounds assay

The inhibitory effect of VOC produced by the bacterial isolates on *S. rolfsii* was assessed using the sealed plate technique (Calvo et al., 2020). A 100 µl aliquot of each bacterial culture (approximately 10^7 CFU/ml) was spread evenly onto NA plates and incubated at 37 °C for 24 h. At the same time, a 5 mm mycelial plug cut from a 3-day-old *S. rolfsii* colony grown on PDA was placed at the center of a fresh PDA plate. After incubation, the lid of the bacterial plate was removed and replaced with the base of the PDA plate containing *S. rolfsii*, ensuring that the agar surfaces did not make contact. The paired plates were sealed tightly with Parafilm™ to prevent VOC leakage. Plates containing S. *rolfsii* alone (without bacterial VOC exposure) served as the control. All paired plates were incubated at 28 ± 2 °C for 3 days. The colony diameter of *S. rolfsii* was measured, and the percentage of mycelial growth inhibition was calculated as described above. Each experiment was performed twice with triplicate in each trial.

2.4. Genome sequencing and BGC profiling

Whole-genome sequencing of R-KT-26 was performed using an Illumina platform. The obtained raw sequencing data were subjected to quality control and trimming prior to *de novo* assembly with Unicycler

(Wick et al., 2017). Genome annotation was conducted using PROKKA for the prediction of protein-coding sequences (CDSs), whereas transfer RNA (tRNA) and ribosomal RNA (rRNA) genes were identified using tRNAscan-SE v2.0 (Chan and Lowe, 2019) and Barrnap, respectively (Seemann, 2014).

To determine the phylogenomic position of R-KT-26, its whole-genome sequence was analyzed together with 20–30 publicly available genomes of closely related *Priestia* species using the AutoMLST2 web server (Alanjary et al., 2019). The uploaded FASTA files were processed through the *de novo* pipeline, in which pairwise genomic distances were estimated using Mash and average nucleotide identity (ANI), followed by the selection of the most closely related reference genomes from the GTDB database. Conserved single-copy marker genes shared among all included taxa were identified, individually aligned, and concatenated into a supermatrix for downstream phylogenetic inference.

A maximum-likelihood phylogenomic tree was generated in IQ-TREE using the optimal substitution model automatically selected by AutoMLST2 based on the concatenated core-gene alignment. Statistical support for branching patterns was assessed using 1000 bootstrap replications. The final tree, exported in Newick format, was visualized in FigTree v1.4.4, and the terminal labels were modified to indicate the corresponding species or strain names along with their genome accession numbers.

Furthermore, secondary metabolite biosynthetic gene clusters (BGCs) in R-KT-26 were predicted using antiSMASH v6.0.1 (Blin et al., 2021). The identified clusters were functionally annotated and systematically compared with reference BGCs deposited in the MIBiG database. Similarity levels (high, medium, or low) were assigned based on concordance in gene content and overall cluster architecture, as inferred from the antiSMASH output.

2.5. Culture filtrates antifungal assay

The antifungal activity of culture filtrates (CF) produced by R-KT-26 against *S. rolfsii* was evaluated under both solid and liquid culture conditions using PDA and PDB, respectively. Strain R-KT-26 was grown in NB at 37 °C for 48 h on a rotary shaker (150 rpm). The bacterial culture was centrifuged at 5000 rpm for 15 min, and the resulting supernatant was passed through a 0.22 μm syringe filter to obtain sterile CF.

PDA assay, double-strength PDA was prepared to compensate for dilution after mixing with CF. The medium was autoclaved at 121 °C for 15 min and cooled to approximately 60 °C before adding R-KT-26 CF to achieve final concentrations of 1%, 15%, 30%, 45%, and 60% (v/v) in a total volume of 10 mL per plate. The mixture was thoroughly blended and poured into sterile Petri dishes. Plates without CF served as the control. A 5 mm diameter mycelial plug taken from a 3-day-old *S. rolfsii* colony was placed at the center of each plate, and all plates were incubated at 28 ± 2 °C for 2 days. The colony diameter was measured, and the percentage of mycelial growth inhibition was calculated as previously described.

In the PDB assay, R-KT-26 CF was incorporated into sterile PDB to obtain final concentrations of 1%, 15%, 30%, 45%, and 60% (v/v), with a total volume of 10 mL per flask. A 5-mm mycelial plug of *S. rolfsii* was inoculated into each flask and incubated under static conditions at 28 ± 2 °C for 2 days. Following incubation, the mycelial biomass was harvested by filtration, dried at 60 °C to constant weight, and weighed. Fungal growth inhibition was determined relative to the control (PDB without CF). Ponderal inhibition of fungal growth was determined based on mycelial dry weight using the following equation: Inhibition (%) = $[(W_1 - W_2)/W_1] \times 100$, where W_1 corresponds to the dry biomass of the untreated control, and W_2 represents the dry biomass obtained from CF-treated samples.

Each experiment in both PDA and PDB assays was conducted twice with three replicates per treatment.

2.6. Culture filtrates broad-spectrum activity

The broad-spectrum antifungal activity of CF produced by R-KT-26 at 60% (v/v) was evaluated against ten phytopathogenic fungi: *S. commune*, *L. theobromae*, *P. salaccae*, *C. oryzae*, *A. parasiticus*, *A. flavus*, *R. solani*, *C. cassiicola*, *C. musae*, and *F. incarnatum*. Each fungal isolate was inoculated into PDB containing 60% (v/v) CF, while PDB without CF served as the control. The cultures were incubated at 28 ± 2 °C on a rotary shaker at 150 rpm for 3–7 days, depending on the growth rate of each fungus. After incubation, the mycelial biomass was harvested by filtration, dried to constant weight, and used to determine fungal growth. The percentage inhibition of mycelial growth was calculated based on dry weight as described in the previous section. Each experiment was performed twice with triplicate in each trial.

2.7. Culture filtrates compared with synthetic fungicides

The antifungal efficacy of R-KT-26 CF at 45% and 60% (v/v) was compared with various concentrations (0.1%, 0.2%, 0.4%, 0.6%, 0.8%, and 1.0% v/v) of three commercial fungicides—prochloraz, azoxystrobin, and propiconazole—against the mycelial growth and sclerotia formation of *S. rolfsii*.

For the mycelial growth assay, each treatment (CF or synthetic fungicide) was incorporated into molten PDA to obtain a final volume of 10 mL per plate, which was then poured into sterile Petri dishes. PDA plates without any treatment served as controls. A 5-mm mycelial plug from a 3-day-old *S. rolfsii* culture grown on PDA was placed at the center of each plate. All plates were incubated at 28 ± 2 °C for 3 days, after which colony diameters were measured. The percentage of mycelial growth inhibition was calculated as previously described. Each experiment was performed twice with triplicate in each trial.

For the sclerotia formation assay, the procedure was similar to that of the mycelial growth test, except that nine uniform sclerotia of *S. rolfsii* were placed on each plate instead of a mycelial plug. After incubation at 28 ± 2 °C, sclerotia germination was observed at 16 h and 40 h. Each experiment was conducted twice with three replicates per treatment, using nine sclerotia per replicate.

2.8. Heat- and dilution-stable culture filtrates assay

The effects of diluted and autoclaved R-KT-26 CF on the germination of *S. rolfsii* sclerotia were evaluated using 24-well microplates. Treatments included undiluted CF and serial dilutions at 1:10, 1:100, and 1:1,000, prepared by mixing the CF with PDB. Each well received 1 mL of the respective dilution. For the heat-treated group, 1 mL of autoclaved CF (121 °C for 15 min) was added to separate wells. Nine surface-sterilized sclerotia were placed in each well. Wells containing PDB without CF served as controls. The plates were incubated at 28 ± 2 °C, and sclerotial germination was recorded at 16 h and 40 h of incubation. Each experiment consisted of nine sclerotia per well with three replicates per trial.

2.9. LC–QTOF–MS bioactive metabolite profiling

The CF of R-KT-26 was analyzed for metabolite profiling to explore potential antifungal compounds using a liquid chromatography–quadrupole time-of-flight mass spectrometry system (LC–QTOF–MS; Agilent 1290 Infinity II LC coupled with a 6545 Q-TOF, Agilent Technologies, USA). Sample preparation was performed following previously described procedures.

Chromatographic separation was achieved using a Zorbax Eclipse Plus C18 Rapid Resolution HD column (150 × 2.1 mm, 1.8 μm; Agilent) maintained at 25 °C. The mobile phases included water containing 0.1% acetic acid (solvent A) and LC–MS grade methanol (solvent B), with a flow rate of 0.2 mL/min. The gradient elution started at 95% A for 2 min, followed by a linear decrease to 0% A over 40 min, held until 45 min,

and then returned to the initial condition for re-equilibration. A fixed injection volume of 10 μL was applied.

Mass detection was performed in both positive and negative electrospray ionization modes (+ESI and –ESI) under AutoMS/MS acquisition. Spectral data were collected over an *m/z* range of 100–1200 for full scan, while fragmentation spectra were obtained within *m/z* 50–1200 using collision energies of 10, 20, and 40 V. Mass accuracy was continuously calibrated using reference ions at *m/z* 121.0509 and 922.0098 in positive mode, and *m/z* 112.9856 and 1033.9881 in negative mode. Putative metabolite identification was conducted by comparing accurate mass and MS/MS fragmentation patterns with the METLIN database through MassHunter PCD/PCDL software (version 8.0).

2.10. Greenhouse and field evaluation of disease control

2.10.1. Seed germination assay

One hundred chili pepper seeds were soaked with 1 mL of each treatment: (1) sterile distilled water (control), (2) bacterial cells of R-KT-26 (1×10^7 CFU/mL), (3) culture broth of R-KT-26, and (4) R-KT-26 CF. The treated seeds were placed in sterile plastic containers with moist conditions ($19.2 \times 28.0 \times 10.9$ cm^3). The potential phytotoxicity of R-KT-26 was assessed based on the percentage of seed germination, stem length, root length, and fresh weight of seedlings after 10 days of incubation. Each experiment was conducted twice, with three replicates of 100 seeds per trial.

2.10.2. Disease control

Greenhouse and field trials were conducted to evaluate the efficacy of R-KT-26 in suppressing southern blight caused by *S. rolfsii*. Greenhouse experiments were performed in plastic baskets (36×50 cm^2) containing 1 kg of autoclaved soil mixed with *S. rolfsii* inoculum at 15 g/kg. Chili pepper seeds were coated for 1 h with one of the following treatments: (1) sterile NB medium, (2) bacterial cells of R-KT-26 (1×10^7 CFU/mL), (3) culture broth of R-KT-26, (4) R-KT-26 CF, (5) prochloraz, or (6) propiconazole. Treated seeds were sown in the baskets at 100 seeds per replicate. Seven days after sowing, 30 mL of the respective treatment was applied again by spraying onto each basket. Seedling survival was recorded 30 days after sowing. All treatments were performed in three replicates.

Field experiments were conducted at the Plant Research Station, Songkhla Rajabhat University, Thailand (7.16585° N, 100.61294° E). The climate is classified as tropical monsoon (Köppen–Geiger: Am), with warm temperatures throughout the year (annual average ~27–28 °C) and high annual rainfall (~1900–2000 mm) (Peel et al., 2007). The soil used in plastic bags for the field trials was loamy, with a pH of 6.5 and 2.1% organic matter content. Fifteen-day-old seedlings were transplanted into plastic bags (6×14 cm^2) containing 3 kg of non-sterilized soil, one seedling per bag, arranged following a natural layout. Treatments were applied as described for the greenhouse experiment. Thirty days after transplanting, 1 g of *S. rolfsii* inoculum was applied around each seedling (~2 cm from the base). For each treatment, 10 mL of the biological or chemical solution was applied to the base of each seedling immediately after inoculation and again three days later.

Seven days after inoculation, disease severity was assessed for individual plants using a 0–5 scale, where 0 = healthy plant, 1 = presence of lesions without leaf wilting, 2 = presence of lesions with 1–2 wilted leaves, 3 = more than 2 wilted leaves, 4 = plant damped-off, and 5 = dead plant. The disease severity index (DSI) was calculated using the following formula: DSI (%) = [Σ (disease rating × number of plants in that rating)/(total number of plants × maximum disease rating)] × 100. The percentage of disease reduction was calculated as: Disease reduction (%) = [(DSI of control − DSI of treatment)/DSI of control] × 100. These calculations were performed according to Chiang et al. (2017). Each treatment included three replicates, with six bags per replicate, totaling 18 bags.

2.11. Mycolytic activity and mode of action

2.11.1. Assessment of bacterial growth on fungal biomass

To assess whether the bacterial R-KT-26 can utilize *S. rolfsii* mycelial biomass as a nutrient source and thereby enhance its population, an assay was performed with modifications from Mannaa et al. (2023). Briefly, *S. rolfsii* was cultured in PDB at 28 ± 2 °C on a rotary shaker (150 rpm) for 2 days to generate mycelial biomass. The mycelia were aseptically harvested, washed twice with sterile distilled water to remove residual fungal metabolites, and weighed.

Bacterial suspensions of R-KT-26 were prepared from overnight cultures and adjusted to an OD_{600} of 0.6. The assay was conducted in NB diluted 1:1000 (v/v) with sterile distilled water. Two experimental setups were established: R-KT-26 co-incubated with fungal mycelia (+fungi) and R-KT-26 alone (-fungi). Each tube contained a total volume of 3 mL, comprising 6 mg of fungal mycelia and 100 μL of bacterial suspension. Tubes were incubated at 28 ± 2 °C on a rotary shaker (150 rpm) for 2 days. After incubation, 100 μL of each culture was plated onto NA after appropriate serial dilutions, and colony-forming units (CFUs) were enumerated following 2 days of incubation at 37 °C. Each experiment was performed twice with triplicate in each trial.

2.11.2. Antifungal mechanism assay

To investigate the mechanisms by which R-KT-26 CF exert antifungal activity against *S. rolfsii*, mycelial biomass was prepared as previously described. Approximately 1 g (wet weight) of clean mycelia was resuspended in 10 mL of PDB supplemented with 60% (v/v) R-KT-26 CF, while PDB without CF served as the control. The suspensions were incubated at 28 ± 2 °C for 3 days.

After incubation, the mycelial samples were prepared for enzymatic and non-enzymatic defense response analyses. Briefly, fungal biomass from both treated and control groups was homogenized in 3 mL of phosphate-buffered saline (PBS, 100 mM, pH 7.4) and centrifuged at 8000 rpm for 10 min at 4 °C. The resulting supernatants were used for downstream biochemical analyses (Das et al., 2020). The resulting supernatant was collected for analysis of oxidative stress and antioxidant defense responses. Intracellular reactive oxygen species (ROS) were quantified using 2′,7′-dichlorodihydrofluorescein diacetate (DCFH-DA) with excitation/emission wavelengths of 485/530 nm, and DCF concentrations were calculated based on a standard curve (Keston and Brandt, 1965). Catalase (CAT) activity was assayed according to Beers and Sizer (1952) and expressed as units per minute per milligram of protein, using a molar extinction coefficient of 43.6 M^{-1} cm^{-1} (Das et al., 2020). Superoxide dismutase (SOD) activity was determined via the quercetin auto-oxidation method (Kostyuk and Potapovich, 1989) and expressed as inhibition of quercetin oxidation per milligram of protein (Das et al., 2020). Reduced glutathione (GSH) and oxidized glutathione (GSSG) levels were measured after homogenization in phosphate buffer containing EDTA and metaphosphoric acid. GSH fluorescence was measured at excitation 350 nm/emission 420 nm, while GSSG levels were determined following reaction with N-ethylmaleimide (NEM) and o-phthalaldehyde (OPA) (Kostyuk and Potapovich, 1989). Total protein content was determined according to Lowry et al. (1951). Each experiment was performed twice with triplicate in each trial.

2.12. Statistical analysis

Data were analyzed using IBM SPSS Statistics version 26 (IBM Corp., Armonk, NY, USA). One-way analysis of variance (ANOVA) was performed, and the normality of the data was verified. Tukey's Honestly Significant Difference (HSD) test ($p < 0.05$) was applied to identify statistically significant differences between treated samples and the untreated control.

3. Results

3.1. Isolation of antagonistic bacteria

A total of 13 bacterial isolates were screened for antifungal activity against *S. rolfsii* using both direct dual culture and indirect VOC assays (Supplementary Table S1). In the dual culture assay, radial mycelial growth differed significantly among treatments ($p < 0.05$). Ten isolates inhibited mycelial growth by more than 67% compared with the control, with isolates R-KT-01, R-KT-04, R-KT-26, R-KT-27, and R-KT-36 achieving complete inhibition (100%) (Supplementary Fig. S1). In the VOC assay, all isolates produced VOC, with inhibition ranging from 2.22% to 34.44%. The strongest VOC-mediated inhibition was observed for R-KT-08 (34.44%), followed by R-KT-26 (29.26%) ($p < 0.05$). Overall, inhibition in the VOC assay was lower than in the dual culture assay, suggesting that non-volatile compounds play a dominant role in suppressing *S. rolfsii* growth. Based on these results, isolate R-KT-26 was selected for further study due to its superior antifungal activity, demonstrating both volatile- and non-volatile-mediated inhibition.

3.2. Genome sequencing and BGC profiling

Whole-genome sequencing of R-KT-26 was performed on the Illumina platform, and the resulting reads were assembled *de novo* using Unicycler (Supplementary Table S2). The assembled genome comprised a single circular chromosome with a total length of 5,468,977 bp and a GC content of 37.7%. Visualization of the genome using the circlize package demonstrated an organized chromosomal structure with genomic elements distributed throughout the chromosome. Genome annotation identified 5652 predicted protein-coding genes (CDSs), along with 58 tRNA genes and four rRNA operons. The circular genomic architecture of R-KT-26 is shown in Supplementary Fig. S2.

Phylogenomic placement of R-KT-26 was inferred using AutoMLST2 based on concatenated core-gene sequences. The resulting analysis assigned R-KT-26 to the *Priestia aryabhattai* lineage, where it grouped together with the reference genome *P. aryabhattai* GCF_009497655, forming a clearly supported monophyletic cluster. The maximum-likelihood phylogenomic tree reconstructed by AutoMLST2 and visualized with FigTree v1.4.4 exhibited a consistent branching pattern with strong bootstrap support across the principal nodes (Supplementary Fig. S3). Collectively, these results confirm the taxonomic classification of strain R-KT-26 as *P. aryabhattai*.

Analysis of the genome of *P. aryabhattai* R-KT-26 using antiSMASH v6.0.1 identified seven putative BGCs associated with secondary metabolite production (Supplementary Table S3). These BGCs were assigned to diverse biosynthetic categories, including terpenes, ribosomally synthesized and post-translationally modified peptides (RiPPs), siderophores, and type III polyketide synthases (T3PKS). Five of the predicted clusters showed high similarity to previously characterized BGCs deposited in the MIBiG database, whereas two clusters exhibited low similarity to known references. Among the high-similarity clusters, several were related to terpene biosynthesis, including gene clusters associated with sodorifen, biarylitide YYH, and fumihopaside A. In addition, a lassopeptide BGC displaying high similarity to the paeninodin biosynthetic cluster was identified. A nonribosomal-independent siderophore (NI-siderophore) gene cluster related to schizokinen biosynthesis was also detected, indicating the presence of a conserved genetic basis for siderophore production in strain R-KT-26. In contrast, two predicted BGCs showed low similarity to known MIBiG entries. These included a T3PKS cluster associated with benzoquinone-related compounds and a terpene cluster related to carotenoid biosynthesis. The reduced similarity of these clusters to previously characterized BGCs may indicate sequence divergence or structural variation in the corresponding biosynthetic pathways.

3.3. Culture filtrates antifungal assay

Supplementary Table S4 summarizes the inhibitory effects of different concentrations (1–60% v/v) of R-KT-26 CF on the growth of *S. rolfsii* under solid (PDA; Table S4A) and liquid (PDB; Table S4B) culture conditions. On PDA, antifungal activity increased in a concentration-dependent manner. Colony diameter in the control averaged 5.15 cm, whereas progressive growth reduction was observed with increasing CF concentrations ($p < 0.05$), reaching complete inhibition at 60% (v/v). Notable growth suppression (~59% inhibition) occurred at 30% and 45% CF. In PDB, R-KT-26 CF exhibited markedly stronger antifungal activity. The control showed a mean mycelial dry weight of 142.63 mg, while growth was almost completely suppressed at 30% (v/v), with only 0.23 mg remaining (99.84% inhibition). No significant differences ($p > 0.05$) were detected among the 30%, 45%, and 60% treatments. Overall, R-KT-26 CF showed substantial antifungal activity in both solid and liquid systems.

3.4. Culture filtrates broad-spectrum activity

R-KT-26 CF exhibited strong broad-spectrum antifungal activity against ten plant pathogenic fungi (Fig. 1). Significant reductions in mycelial growth (Fig. 1A and C), accompanied by increased inhibition percentages (Fig. 1B), were observed in all treated groups compared with the controls. Among the tested fungi, *A. flavus* showed the highest inhibition rate (95.47%), whereas *F. incarnatum* exhibited the lowest (80.45%); inhibition of the remaining species ranged from 81.43% to 93.99%. Statistical analysis indicated that inhibition of *A. flavus* was significantly ($p < 0.05$) higher than that of *F. incarnatum* and *P. salaccae*, while no significant differences ($p > 0.05$) were detected among the other fungi. Overall, these results demonstrate that R-KT-26 CF possess potent broad-spectrum antifungal activity against diverse plant pathogens.

3.5. Culture filtrates compared with synthetic fungicides

Supplementary Tables S5 and S6 present the comparative efficacy of R-KT-26 CF and three commercial fungicides against *S. rolfsii*. Significant differences ($p < 0.05$) were observed among treatments in terms of radial growth and growth inhibition. The 60% (v/v) R-KT-26 CF completely suppressed mycelial growth (100% inhibition), comparable to prochloraz (≥0.2% w/v) and propiconazole (≥0.1% w/v), while azoxystrobin showed partial, dose-dependent inhibition (59.81–74.17%) (Table S5).

For sclerotia formation, control treatments germinated 55.89% at 16 h and reached 100% at 40 h. In contrast, both 45% and 60% R-KT-26 CF, as well as all tested fungicide concentrations, achieved complete suppression (0% germination) throughout the observation period (Table S6). Overall, these findings demonstrate that CF are as effective as commercial fungicides in inhibiting both mycelial growth and sclerotia germination of *S. rolfsii* under *in vitro* conditions, underscoring their potential as a promising biocontrol alternative.

3.6. Heat- and dilution-stable culture filtrates assay

Significant ($p < 0.05$) inhibition of sclerotial germination was observed for all dilutions and autoclaved R-KT-26 CF in PDB medium at both 16 h and 40 h (Fig. 2). As shown in Fig. 2A, undiluted CF completely inhibited sclerotial germination (100%) at both time points, indicating strong antifungal activity. The 1:10 dilution also resulted in complete inhibition throughout the incubation period. In contrast, partial inhibition was observed with the 1:100 dilution, with germination increasing from 0% at 16 h to 44.44% at 40 h. The 1:1000 dilution showed limited antifungal activity, allowing 37.04% germination at 16 h and 92.59% at 40 h. Notably, autoclaving the CF at 121 °C for 15 min did not reduce antifungal efficacy, as complete inhibition of

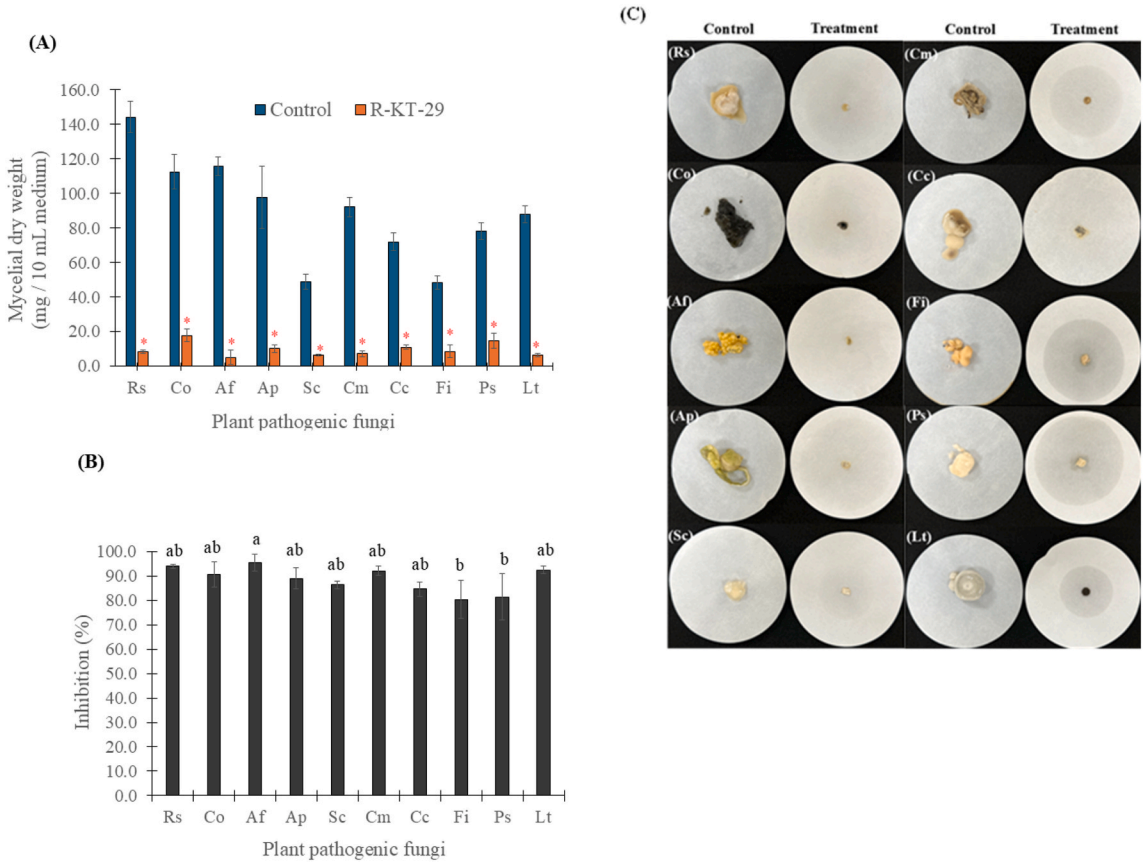

Fig. 1. Broad-spectrum antifungal activity of *P. aryabhattai* R-KT-26 culture filtrates against ten plant pathogenic fungi. **(A)** Mycelial growth, **(B)** percentage of growth inhibition, and **(C)** colony morphology of *R. solani* (Rs), *C. oryzae* (Co), *A. flavus* (Af), *A. parasiticus* (Ap), *S. commune* (Sc), *C. musae* (Cm), *C. cassiicola* (Cc), *F. incarnatum* (Fi), *P. salaccae* (Ps), and *L. theobromae* (Lt) cultured in PDB at 28 ± 2 °C for 3–7 days.

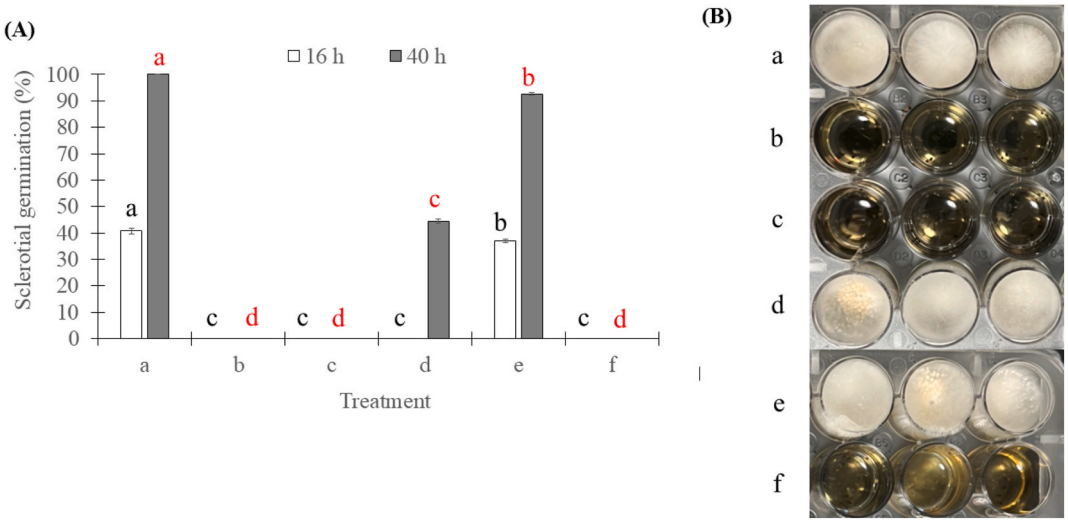

Fig. 2. Antifungal activity of *P. aryabhattai* R-KT-26 culture filtrates (CF) against *S. rolfsii*. **(A)** Percent sclerotial germination in PDB. **(B)** Morphological observation of sclerotial germination in a well plate after incubation at 28 ± 2 °C for 40 h. Values followed by the same letter are not significantly different according to ANOVA and Tukey's HSD test ($p > 0.05$). **(a)** *S. rolfsii* alone (control); **(b)** untreated R-KT-26 CF; **(c)** CF diluted 1/10; **(d)** CF diluted 1/100; **(e)** CF diluted 1/1000; **(f)** autoclaved CF.

sclerotial germination was maintained, suggesting that the active metabolites produced by R-KT-26 are heat-stable. Morphological changes in sclerotial germination under different treatments are shown in Fig. 2B.

3.7. LC–QTOF–MS bioactive metabolite profiling

The secondary metabolites present in the CF of *P. aryabhattai* R-KT-26 were profiled using LC–QTOF–MS in two ionization modes, as summarized in Supplementary Tables S7 and S8, with representative

chromatograms shown in Supplementary Fig. S4. A total of 103 and 139 compounds were detected in the negative (−ESI) (Table S7) and positive (+ESI) (Table S8) modes, respectively. The difference in the number of detected compounds between the two modes can be attributed to variations in ionization efficiencies and the chemical properties of the metabolites, with certain compounds preferentially ionized under specific conditions.

Among all detected compounds, 16—including adenine, gln pro leu, ponasteroside A, and a compound putatively annotated as amaranthus saponin I—were detected in both ionization modes, indicating chemical stability under the analytical conditions. In the negative mode, DIMBOA (2,4-dihydroxy-7-methoxy-1,4-benzoxazin-3-one) and valclavam were detected, whereas in the positive mode, aspergillic acid, imazamethabenz, and the putatively annotated amaranthus saponin I were observed. All compound annotations were based on LC–QTOF–MS database matching and should be interpreted with caution, as structurally related metabolites may share similar mass spectral features.

3.8. Greenhouse and field evaluation of disease control

The effects of R-KT-26 and its derivatives on chili pepper seed germination and seedling growth are shown in Supplementary Fig. S5. Seed germination was significantly ($p < 0.05$) enhanced by treatments with bacterial cells and culture broth of R-KT-26 (98%), with no significant ($p > 0.05$) difference between these treatments (Fig. S5A). In contrast, CF and sterile distilled water resulted in lower germination rates (91% and 93%, respectively). Bacterial cells, culture broth, and CF significantly increased stem length compared with the control (26.4–28.05 mm; Fig. S5B), while CF promoted the greatest root length (49.0 mm; Fig. S5C). Fresh weight did not differ significantly among treatments (139.25–150.15 mg; Fig. S5D). Normal seedling morphology was observed in all treatments (Fig. S5E), indicating no phytotoxic effects of R-KT-26 on chili pepper seedlings.

The biocontrol potential of R-KT-26 against southern blight of chili pepper caused by *S. rolfsii* was evaluated under greenhouse and field conditions (Fig. 3). In the greenhouse experiment (Fig. 3A), chili seedlings treated with R-KT-26 cell suspension showed a significantly ($p < 0.05$) higher survival rate (59.00%) than the untreated control (24.33%) and were comparable to prochloraz (60.67%). Treatments with culture broth (54.67%) and propiconazole (52.67%) also resulted in relatively high survival, whereas CF were less effective (34.67%).

Under field conditions (Fig. 3B–D), disease severity was highest in the untreated control (DSI = 73.89%). All treatments significantly ($p < 0.05$) reduced disease severity. Application of R-KT-26 cell suspension (1×10^7 CFU/mL) reduced the DSI to 19.78%, corresponding to a disease reduction of 73.19%, which did not differ significantly ($p > 0.05$) from synthetic fungicide. Culture broth and CF were less effective, with DSI values of 31.11% and 43.33%, respectively. Prochloraz and propiconazole showed the highest efficacy, resulting in the lowest DSI values (13.34% and 11.89%) and the greatest disease reduction (81.88% and 83.91%).

3.9. Mycolytic activity and mode of action

An *in vitro* assay was performed using a nutrient-poor medium (10^{-3} × diluted NB) to investigate the mechanism of action of R-KT-26 against *S. rolfsii* (Fig. 4). When co-cultivated with fungal mycelia, the population of R-KT-26 increased markedly, reaching 7.35 Log CFU/mL, compared with 4.69 Log CFU/mL in the control without fungal biomass. Spotting assays (Fig. 4A) and CFU enumeration (Fig. 4B) consistently demonstrated that R-KT-26 was able to utilize *S. rolfsii* mycelia as a nutrient source.

Oxidative stress associated with the antifungal activity of R-KT-26 CF against *S. rolfsii* was evaluated by analyzing intracellular ROS levels and antioxidant-related parameters (Fig. 4C–H). ROS accumulation increased markedly following exposure to R-KT-26, rising from 10.52 μM/mg protein in the control to 89.62 μM/mg protein in the treated group (Fig. 4C). Correspondingly, SOD and CAT activities were

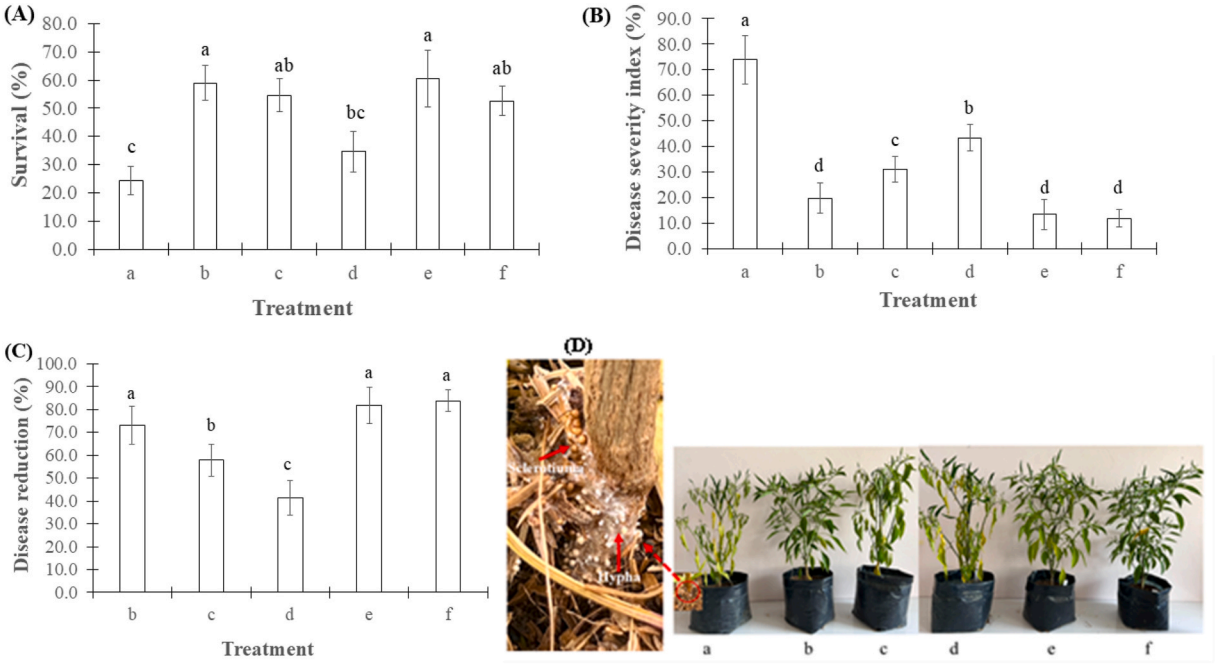

Fig. 3. Combined results of greenhouse and field experiments. **(A)** Percent survival of chili pepper seedlings treated with biological and chemical control agents under greenhouse conditions, 30 days after inoculation with *S. rolfsii*. **(B, D)** Percent disease severity index, and **(C)** percent disease reduction in the field experiment, evaluated 7 days after treatment with biological and chemical control agents. Values represent means of three replicates (±SD), based on 100 chili seeds per treatment in the greenhouse experiment and six chili plants per treatment (18 plants in total) in the field experiment. Values followed by the same letter are not significantly different according to ANOVA and Tukey's HSD test ($p > 0.05$). **(a)** Sterile water control; **(b)** bacterial cells of R-KT-26; **(c)** bacterial broth of R-KT-26; **(d)** culture filtrates of R-KT-26; **(e)** prochloraz; **(f)** propiconazole.

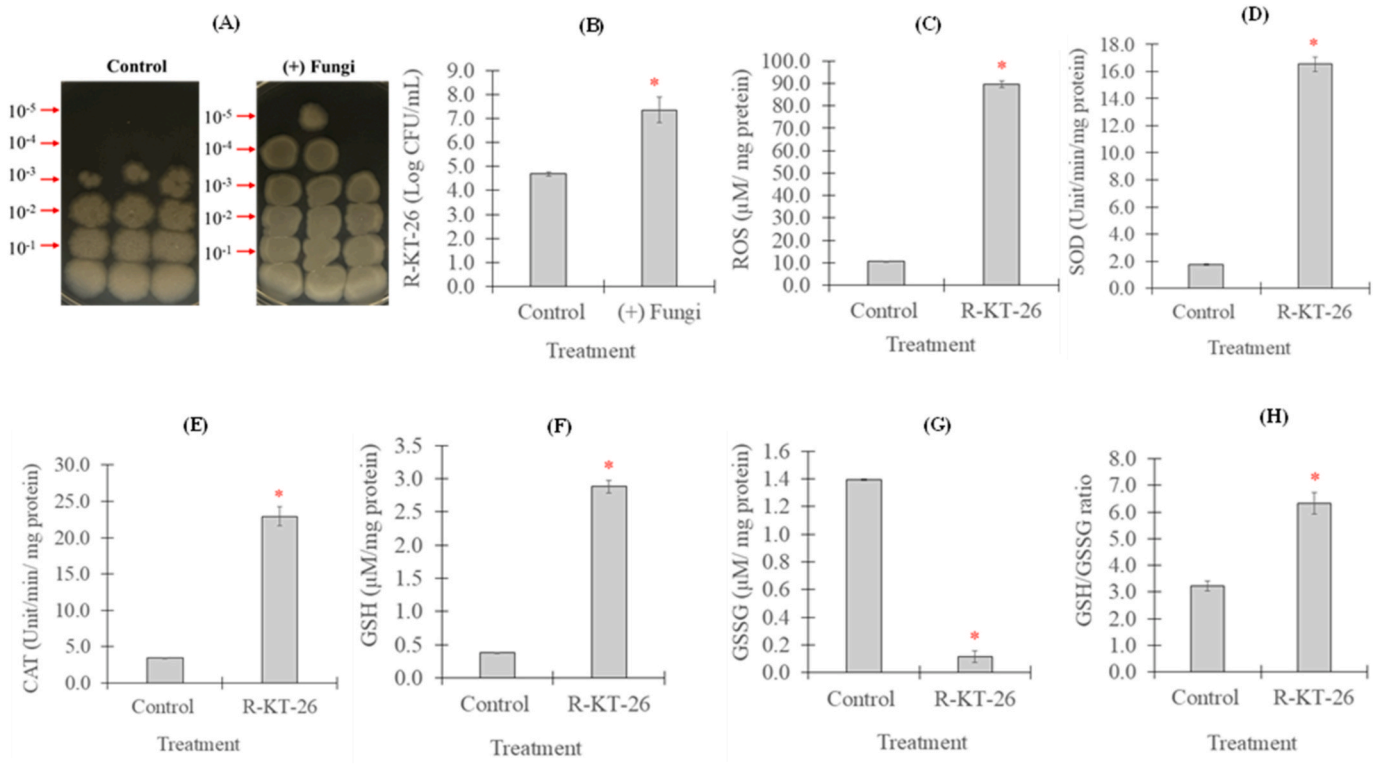

Fig. 4. *In vitro* mycolytic assay and antifungal mechanism of *P. aryabhattai* R-KT-26 against *S. rolfsii*. **(A, B)** Mycolytic assay; **(C)** intracellular reactive oxygen species (ROS) levels; **(D)** superoxide dismutase (SOD) activity; **(E)** catalase (CAT) activity; **(F)** reduced glutathione (GSH) levels; **(G)** oxidized glutathione (GSSG) levels; **(H)** GSH/GSSG ratio.

significantly elevated (Fig. 4D and E). Alterations in the glutathione redox system were also observed, with increased GSH levels, reduced GSSG content, and a significantly higher GSH/GSSG ratio in the treated samples compared with the control (Fig. 4F–H). Collectively, these results indicate that R-KT-26 disrupts redox homeostasis in *S. rolfsii*, accompanied by activation of antioxidant defense responses.

4. Discussion

Beneficial rhizosphere microorganisms are recognized as sustainable alternatives to synthetic pesticides due to their antimicrobial activity against various fungal phytopathogens (Hernández-Rodríguez et al., 2024; Zhu et al., 2025). In this study, rhizosphere-derived antagonistic bacteria suggested variable but significant inhibition of *S. rolfsii*, highlighting the diverse strategies soil bacteria employ for pathogen suppression. Importantly, the strong and consistent inhibitory effects observed across *in vitro*, greenhouse, and field conditions suggest that strain R-KT-26 provides effective pathogen mitigation under multiple experimental systems. Notably, the stronger inhibition observed with diffusible metabolites compared with VOCs suggests that soluble compounds are the primary contributors to antifungal activity, consistent with previous reports on rhizosphere biocontrol agents (Hernández-Rodríguez et al., 2024; Zhu et al., 2025). Similar observations have been reported in *B. subtilis* and related *Priestia* spp., where diffusible secondary metabolites were the main contributors to fungal growth suppression (Caulier et al., 2019; Ruangwong et al., 2022). Importantly, R-KT-26 CF achieved complete inhibition of *S. rolfsii* mycelial growth at 60% (v/v) and fully suppressed sclerotial germination, supporting strong biocontrol potential.

Genomic analysis of *P. aryabhattai* R-KT-26 revealed multiple BGCs associated with terpenes, RiPPs (lassopeptides), siderophores, and type III polyketide synthases, supporting its potential for producing diverse secondary metabolites. The presence of terpene- and RiPP-associated BGCs suggests possible mechanisms such as membrane modulation and stabilization under environmental fluctuations (Caulier et al., 2019), while siderophore-mediated iron sequestration likely limits pathogen access to essential nutrients, aligning with documented cases in other *Bacillus* species (Kumar et al., 2024; Saini et al., 2024). These genomic features provide a functional basis for the observed antifungal activity and support the role of R-KT-26 in sustained pathogen mitigation under nutrient-competitive rhizosphere conditions. Moreover, the identification of numerous putative metabolites in the R-KT-26 CF (103 and 139 compounds by LC–QTOF–MS) provides molecular evidence supporting the antifungal activity predicted from genomic data.

In contrast to previously reported antifungal lipopeptides from *Bacillus* species (Caulier et al., 2019), which typically range from 900 to 1500 Da, most of the metabolites identified in this study had molecular weights below 900 Da. This difference may reflect variations in strain-specific metabolic capabilities and culture conditions. Low-molecular-weight metabolites may exhibit diverse biological activities, including antimicrobial effects, suggesting that compounds other than lipopeptides may contribute to the observed antifungal activity. Importantly, the predominance of low-molecular-weight metabolites may facilitate diffusion and bioavailability within the rhizosphere environment, thereby enhancing their potential contribution to effective pathogen mitigation, as supported by the results obtained under greenhouse and field conditions. Such physicochemical properties may partly explain the strong antifungal efficacy of the culture filtrates observed across multiple experimental systems in this study. Chemical profiling of R-KT-26 CF revealed several putatively identified metabolites, including DIMBOA and amaranthus saponin I, based on LC–QTOF–MS analysis, with compound annotation supported by database matching and literature reports (Yang et al., 2006; Gleńsk et al., 2016; Kudjordjie et al., 2019; Jamiołkowska et al., 2023).

Furthermore, several other low-molecular-weight compounds detected in this study, such as 3,4-methylenedioxybenzoic acid, 4-

hydroxybenzaldehyde, indole, and embelin, have been reported to possess antimicrobial or redox-active properties that may interfere with fungal cell integrity and metabolism (Aziz et al., 1998; Lee and Lee, 2010; Dwivedi and Singh, 2016). The identification of diketopiperazines (e.g., cyclo-ala-pro) and multiple short-chain peptides (e.g., gly-val-pro, pro-val-asn, and valyl-alanine) further supports the presence of bioactive small molecules that may contribute to antifungal activity through signaling interference, membrane disruption, or synergistic interactions (Borthwick, 2012). Organic acids, including citric acid and β-hydroxyisovaleric acid, may also play auxiliary roles by altering local pH and affecting fungal physiological processes (Raaijmakers et al., 2009). Although these compounds have been previously reported in the literature, their presence in this study is based on LC–QTOF–MS annotation and does not confirm their biological origin or antifungal activity. Therefore, these metabolite annotations should be interpreted with caution, and their potential contribution to antifungal activity remains to be experimentally validated.

Nevertheless, the detection of structurally diverse compounds supports the hypothesis that the antifungal activity of R-KT-26 CF is mediated by a complex mixture of metabolites rather than a single dominant compound, which may contribute to its broad-spectrum activity and consistent pathogen mitigation. This interpretation is further supported by the wide range of chemical classes detected, including amino acid derivatives, peptides, phenolic compounds, alkaloid-like molecules, and organic acids, indicating a metabolically versatile system potentially capable of targeting multiple cellular pathways in the pathogen. Similar metabolite-mediated antifungal effects have been reported in other rhizosphere-associated bacteria, where extracellular compounds act synergistically to disrupt fungal growth and physiology (Dutta and Thakur, 2021; Maurya et al., 2024).

In *S. rolfsii*, exposure to these metabolites appears to induce ROS accumulation and disrupt antioxidant systems, as evidenced by altered GSH/GSSG ratios and SOD/CAT activities. Such perturbation of cellular redox homeostasis likely compromises fungal growth and pathogenicity, consistent with previous observations in plant pathogenic fungi where ROS detoxification is critical for survival and virulence (Zhang et al., 2020, 2023; Park and Son, 2024). This oxidative imbalance represents a key mechanistic pathway underlying the antifungal activity of R-KT-26, linking metabolite production to functional pathogen suppression. Collectively, these findings suggest that the antifungal activity of R-KT-26 CF is multifaceted, involving direct growth inhibition, sclerotial suppression, and disruption of oxidative stress management.

Greenhouse and field evaluations further demonstrated the practical effectiveness of R-KT-26, significantly improving seedling survival and reducing disease severity, with levels of disease suppression comparable to the fungicide treatment under the conditions tested. Similar disease suppression has been reported in pepper plants treated with *B. subtilis*, which reduced southern blight severity and enhanced plant defense responses (Moon and Sang, 2024). Likewise, plant growth-promoting rhizobacteria, including *B. megaterium* and *P. fluorescens*, have been shown to improve plant survival and reduce disease severity caused by *S. rolfsii* in chili (Sharf et al., 2021). Consistent with these findings, recent work by Qiu et al. (2024) demonstrated that *S. griseoaurantiacus* XQ-29 effectively suppressed pepper southern blight through multiple mechanisms, including antifungal metabolite production and disruption of pathogen physiology. Importantly, the consistency between laboratory findings and field performance strengthens the reliability of R-KT-26 as a biocontrol agent for real-world pathogen mitigation. Consistent with these findings, other rhizobacterial isolates have also been reported to simultaneously suppress southern blight and promote plant growth in chili under soil conditions. Beyond pathogen suppression, R-KT-26 also promoted chili seed germination and seedling development, suggesting dual functionality in disease control and plant growth promotion, likely associated with phytohormone-like compounds and siderophore production (Glick, 2012; Chen et al., 2022; de Andrade et al., 2023).

Additionally, the observed mycolytic activity, where R-KT-26 associates with fungal hyphae, provides ecological advantages for direct antagonism and bacterial dispersal, consistent with behaviors reported in *Paraburkholderia* spp., *Burkholderia* spp., and *Pseudomonas* spp. (Warmink et al., 2011; Deveau et al., 2018; Mannaa et al., 2023, 2025). This interaction further supports a contact-dependent mechanism contributing to pathogen suppression, complementing the effects of diffusible antifungal metabolites. Taken together, these results indicate that R-KT-26 suppresses *S. rolfsii* through complementary mechanisms—live-cell interaction with hyphae and bioactive culture filtrates—while simultaneously enhancing plant growth.

5. Conclusion

This study shows that a new isolate of *P. aryabhattai* exhibits strong potential as a biological control agent against chili pepper southern blight caused by *S. rolfsii*. The isolate showed pronounced antagonistic activity, effectively inhibiting mycelial growth and sclerotial formation while also promoting early chili seedling growth. Greenhouse and field evaluations further demonstrated consistent practical effectiveness, supporting effective pathogen mitigation under the conditions tested, with performance comparable to commercial fungicides. Mechanistically, antifungal activity appears to be mediated through multiple complementary strategies, including ROS accumulation, disruption of antioxidant and glutathione-based redox homeostasis in the pathogen, and mycolytic activity, whereby the bacterium associates with fungal hyphae to enhance direct antagonism and bacterial dispersal. Genome mining and metabolomic profiling further support the presence of diverse bioactive traits underlying this activity. Importantly, the integration of mechanistic insights with greenhouse and field validation strengthens confidence in the robustness of this strain for pathogen mitigation in practical settings. Collectively, these findings highlight the isolate as a promising, environmentally friendly, and broad-spectrum alternative to synthetic fungicides for managing chili pepper southern blight.

Funding

This research was financially supported by the Fundamental Fund (FF, Grant No. 1/2568), Songkhla Rajabhat University (Grant No. 003/2569), and the National Research Council of Thailand (NRCT, Grant No. N42A680491).

CRediT authorship contribution statement

Wanida Petlamul: Data curation, Formal analysis, Investigation, Writing – original draft, Writing – review & editing. **Sawai Boukaew:** Conceptualization, Data curation, Formal analysis, Funding acquisition, Investigation, Methodology, Project administration, Resources, Software, Supervision, Validation, Visualization, Writing – original draft, Writing – review & editing. **Sudarat Chumjan:** Investigation. **Natthawut Chuaikaeo:** Investigation. **Premmika Tengchiang:** Investigation. **Benjamas Cheirsilp:** Funding acquisition, Writing – review & editing. **Siriporn Yossan:** Data curation, Formal analysis, Writing – review & editing. **Sirasit Srinuanpan:** Writing – review & editing. **Krittin Chumkaew:** Data curation, Formal analysis, Writing – review & editing.

Declaration of competing interest

The authors declare that they have no conflicts of interest, financial or personal, that could have inappropriately influenced the work reported in this study.

Appendix A. Supplementary data

Supplementary data to this article can be found online at https://doi.

org/10.1016/j.rhisph.2026.101335.

Data availability

The authors do not have permission to share data.

References

Alanjary, M., Steinke, K., Ziemert, N., 2019. AutoMLST: an automated web server for generating multi-locus species trees highlighting natural product potential. Nucleic Acids Res. 47 (W1), W276–W282. https://doi.org/10.1093/nar/gkz282.

Ali, A., Javaid, A., Shoaib, A., Khan, I.H., 2020. Effect of soil amendment with *Chenopodium album* dry biomass and two *Trichoderma* species on growth of chickpea var. Noor 2009 in *Sclerotium rolfsii* contaminated soil. Egypt J. Biol. Pest Control 30, 102. https://doi.org/10.1186/s41938-020-00305-1.

Aziz, N.H., Farag, S.E., Mousa, L.A., Abo-Zaid, M.A., 1998. Comparative antibacterial and antifungal effects of some phenolic compounds. Microbios 93 (374), 43–54.

Beers, R.F., Sizer, I.W., 1952. A spectrophotometric method for measuring the breakdown of hydrogen peroxide by catalase. J. Biol. Chem. 195, 133–140.

Blin, K., Shaw, S., Kloosterman, A.M., Charlop-Powers, Z., van Wezel, G.P., Medema, M. H., Weber, T., 2021. antiSMASH 6.0: improving cluster detection and comparison capabilities. Nucleic Acids Res. 49 (W1), W29–W35. https://doi.org/10.1093/nar/gkab335.

Borthwick, A.D., 2012. 2,5-Diketopiperazines: synthesis, reactions, medicinal chemistry, and bioactive natural products. Chem. Rev. 112 (7), 3641–3716.

Boukaew, S., Kumla, J., Suwannarach, N., 2024. *Peniophora salaccae* sp. nov. (Russulales, basidiomycota), a snake fruit (*Salacca zalacca*) pathogen from southern Thailand. Phytotaxa 662 (2), 137–149. https://doi.org/10.11646/phytotaxa.662.2.2.

Calvo, H., Mendiara, I., Arias, E., Blanco, D., Venturini, M.E., 2020. Antifungal activity of the volatile organic compounds produced by *Bacillus velezensis* strains against postharvest fungal pathogens. Postharvest Biol. Technol. 166, 111208. https://doi.org/10.1016/j.postharvbio.2020.111208.

Caulier, S., Nannan, C., Gillis, A., Licciardi, F., Bragard, C., Mahillon, J., 2019. Overview of the antimicrobial compounds produced by members of the *Bacillus subtilis* group. Front. Microbiol. 10, 302. https://doi.org/10.3389/fmicb.2019.00302.

Ceresini, P.C., Silva, T.C., Vicentini, S.N.C., Júnior, R.P.L., Moreira, S.I., Castro-Ríos, K., Garcés-Fiallos, F.R., Krug, L.D., de Moura, S.S., da Silva, A.G., Custódio, A.A.P., de Mio, L.L.M., Gasparoto, M.C.G., Portalanza, D., Cintra de Jesus Júnior, W., 2024. Strategies for managing fungicide resistance in the Brazilian tropical agroecosystem: safeguarding food safety, health, and the environmental quality. Trop. plant pathol 49, 36–70. https://doi.org/10.1007/s40858-023-00632-2.

Chan, P.P., Lowe, T.M., 2019. tRNAscan-SE: searching for tRNA genes in genomic sequences. Methods Mol. Biol. 1962, 1–14. https://doi.org/10.1007/978-1-4939-9173-0_1.

Chen, Z., Zhou, W., Sui, X., Xu, N., Zhao, T., Guo, Z., Niu, J., Wang, Q., 2022. Plant growth-promoting rhizobacteria with ACC deaminase activity enhance maternal lateral root and seedling growth in switchgrass. Front. Plant Sci. 12, 800783. https://doi.org/10.3389/fpls.2021.800783.

Chiang, K.-S., Liu, H.-I., Tsai, J.-W., Tsai, J.-R., Bock, C.H., 2017. A discussion on disease severity index values. Part II: using the disease severity index for null hypothesis testing. Ann. Appl. Biol. 171, 490–505. https://doi.org/10.1111/aab.12396.

Das, S., Singh, V.K., Dwivedy, A.K., Chaudhari, A.K., Dubey, N., 2020. *Myristica fragrans* essential oil nanoemulsion as novel green preservative against fungal and aflatoxin contamination of food commodities with emphasis on biochemical mode of action and molecular docking of major components. LWT–Food Sci. Technol. 130, 109495. https://doi.org/10.1016/j.lwt.2020.109495.

de Andrade, L.A., Santos, C.H.B., Frezarin, E.T., Sales, L.R., Rigobelo, E.C., 2023. Plant growth-promoting rhizobacteria for sustainable agricultural production. Microorganisms 11, 1088. https://doi.org/10.3390/microorganisms11041088.

Deveau, A., Bonito, G., Uehling, J., Paoletti, M., Becker, M., Bindschedler, S., Hacquard, S., Hervé, V., Labbé, J., Lastovetsky, O.A., Mieszkin, S., Millet, L.J., Vajna, B., Junier, P., Bonfante, P., Krom, B.P., Olsson, S., van Elsas, J.D., Wick, L.Y., 2018. Bacterial–fungal interactions: ecology, mechanisms and challenges. FEMS (Fed. Eur. Microbiol. Soc.) Microbiol. Rev. 42, 335–352. https://doi.org/10.1093/femsre/fuy008.

Dutta, J., Thakur, D., 2021. Diversity of culturable bacteria endowed with antifungal metabolites biosynthetic characteristics associated with tea rhizosphere soil of Assam, India. BMC Microbiol. 21, 216. https://doi.org/10.1186/s12866-021-02278-z.

Dwivedi, D., Singh, V., 2016. Effects of the natural compounds embelin and piperine on the biofilm-producing property of *Streptococcus mutans*. J. Tradit. Complement. Med. 6 (1), 57–61. https://doi.org/10.1016/j.jtcme.2014.11.025.

García-Montelongo, A.M., Montoya-Martínez, A.C., Morales-Sandoval, P.H., Parra-Cota, F.I., de los Santos-Villalobos, S., 2023. Beneficial microorganisms as a sustainable alternative for mitigating biotic stresses in crops. Stresses 3, 210–228. https://doi.org/10.3390/stresses3010016.

Gleńsk, M., Gajda, B., Franiczek, R., Krzyżanowska, B., Biskup, I., Włodarczyk, M., 2016. *In vitro* evaluation of the antioxidant and antimicrobial activity of DIMBOA [2,4-dihydroxy-7-methoxy-2H-1,4-benzoxazin-3(4H)-one]. Nat. Prod. Rep. 30, 1305–1308. https://doi.org/10.1080/14786419.2015.1054284.

Glick, B.R., 2012. Plant growth-promoting bacteria: mechanisms and applications. Scientifica (Cairo) 2012, 963401. https://doi.org/10.6064/2012/963401.

Hernández-Rodríguez, M., Jasso-de Rodríguez, D., Hernández-Castillo, F.D., Moggio, I., Arias, E., Valenzuela-Soto, J.H., Flores-Olivas, A., 2024. The rhizobacterium *Bacillus amyloliquefaciens* MHR24 has biocontrol ability against fungal phytopathogens and promotes growth in *Arabidopsis thaliana*. Microorganisms 12, 2380. https://doi.org/10.3390/microorganisms12112380.

Jamiołkowska, A., Skwaryło-Bednarz, B., Kowalski, R., Yildirim, I., Patkowska, E., 2023. Antifungal potency of amaranth leaf extract: an *in vitro* study. Plants 12, 1723. https://doi.org/10.3390/plants12081723.

Javaid, A., Ali, A., Khan, I.H., Ferdosi, M.F.H., 2023. Leaves of *Chenopodium album* as source of natural fungicides against *Sclerotium rolfsii*. Arab. J. Chem. 16, 104677. https://doi.org/10.1016/j.arabjc.2023.104677.

Jia, S., Song, C., Dong, H., Yang, X.J., Li, X.H., Ji, M.S., Chu, J., 2023. Evaluation of efficacy and mechanism of *Bacillus velezensis* CB13 for controlling peanut stem rot caused by *Sclerotium rolfsii*. Front. Microbiol. 14, 1111965. https://doi.org/10.3389/fmicb.2023.1111965.

Jia, Y., Wen, R., Liang, C., Lan, X., Mao, T., Xing, D., Lin, W., 2026. Enhanced pepper resistance to *Sclerotium rolfsii* through root development and enzyme modulation by hexaconazole and azoxystrobin. Plant Direct 10, e70136. https://doi.org/10.1002/pld3.70136.

Keston, A.S., Brandt, R., 1965. The fluorometric analysis of ultramicro quantities of hydrogen peroxide. Anal. Biochem. 11, 1–5.

Kostyuk, V.A., Potapovich, A.I., 1989. Superoxide-driven oxidation of quercetin and a simple sensitive assay for determination of superoxide dismutase. Biochem. Int. 19, 1117–1124.

Kudjordjie, E.N., Sapkota, R., Steffensen, S.K., Fomsgaard, I.S., Nicolaisen, M., 2019. Maize synthesized benzoxazinoids affect the host associated microbiome. Microbiome 7, 59. https://doi.org/10.1186/s40168-019-0677-7.

Kumar, R., Singh, A., Shukla, E., Singh, P., Khan, A., Singh, N.K., Srivastava, A., 2024. Siderophore of plant growth promoting rhizobacterium origin reduces reactive oxygen species mediated injury in *Solanum* spp. caused by fungal pathogens. J. Appl. Microbiol. 135. https://doi.org/10.1093/jambio/lxae036 lxae036.

Lee, J.-H., Lee, J., 2010. Indole as an intercellular signal in microbial communities. FEMS Microbiol. Rev. 34 (4), 426–444.

Li, C., Zhu, H., Li, C., Qian, H., Yao, W., Guo, Y., 2021. The present situation of pesticide residues in China and their removal and transformation during food processing. Food Chem. 354, 129552. https://doi.org/10.1016/j.foodchem.2021.129552.

Li, L., Wang, J., Liu, D., Li, L., Zhen, J., Lei, G., Wang, B., Yang, W., 2023. The antagonistic potential of peanut endophytic bacteria against *Sclerotium rolfsii* causing stem rot. Braz. J. Microbiol. 54, 361–370. https://doi.org/10.1007/s42770-022-00896-x.

Lowry, O.H., Rosebrough, N.J., Farr, A.L., Randall, R.J., 1951. Protein measurement with the Folin phenol reagent. J. Biol. Chem. 193, 265–275.

Mannaa, M., Han, G., Jeong, T., Kang, M., Lee, D., Jung, H., Seo, Y.-S., 2023. Taxonomy-guided selection of *Paraburkholderia busanensis* sp. Nov.: a versatile biocontrol agent with mycophagy against *Colletotrichum scovillei* causing pepper anthracnose. Microbiol. Spectr. 1. https://doi.org/10.1128/spectrum.02426-23 e02426-23.

Mannaa, M., Jung, T., Kim, A., Lee, D., Seo, Y.-S., 2025. Characterization of *Lasiodiplodia brasiliensis* causing banana black rot in Korea and its biocontrol by *Paraburkholderia busanensis* P39 through volatile-mediated microbiome modulation. Postharvest Biol. Technol. 227, 113621. https://doi.org/10.1016/j.postharvbio.2025.113621.

Maurya, S., Thakur, R., Vighnesh, R., Suresh, S., Dang, A., Raj, D., Srivastava, S., 2024. Eco-friendly management of plant pathogens through secondary metabolites released by fluorescent pseudomonads. J. Pure Appl. Microbiol. 18, 1471–1488. https://doi.org/10.22207/JPAM.18.3.40.

Meena, P.N., Meena, A.K., Tiwari, R.K., Lal, M.K., Kumar, R., 2024. Biological control of stem rot of groundnut induced by *Sclerotium rolfsii* sacc. Pathogens 13, 632. https://doi.org/10.3390/pathogens13080632.

Moon, H.J., Sang, M.K., 2024. Biocontrol of Southern blight caused by *Sclerotium rolfsii* in pepper plants using *Bacillus subtilis* GJ6-14. Res. Plant Dis. 30, 181–188. https://doi.org/10.5423/RPD.2024.30.2.181.

Pal, D.C., Khan, S.N., Karim, M.M., 2025. Draft genome sequence and annotation of *Priestia aryabhattai* MS3, a salt-tolerant plant growth-promoting rhizobacterium. Microbiol. Resour. Announc. 14. https://doi.org/10.1128/mra.00026-25 e00026-25.

Park, J., Son, H., 2024. Antioxidant systems of plant pathogenic fungi: functions in oxidative stress response and their regulatory mechanisms. Plant Pathol. J. 40, 235–250. https://doi.org/10.5423/PPJ.RW.01.2024.0001.

Peel, M.C., Finlayson, B.L., McMahon, T.A., 2007. Updated world map of the Köppen–geiger climate classification. Hydrol. Earth Syst. Sci. 11, 1633–1644. https://doi.org/10.5194/hess-11-1633-2007.

Qiu, Z.L., Liu, S.D., Li, X.G., Zhong, J., Zhu, J.Z., 2024. Identification and mechanism characterization of *Streptomyces griseoaurantiacus* XQ-29 with biocontrol ability against pepper southern blight caused by *Sclerotium rolfsii*. Pestic. Biochem. Physiol. 202, 105956. https://doi.org/10.1016/j.pestbp.2024.105956.

Raaijmakers, J.M., Paulitz, T.C., Steinberg, C., Alabouvette, C., Moënne-Loccoz, Y., 2009. The rhizosphere: a playground and battlefield for soilborne pathogens and beneficial microorganisms. Plant Soil 321 (1–2), 341–361. https://doi.org/10.1007/s11104-008-9568-6.

Ruangwong, O.-U., Kunasakdakul, K., Chankaew, S., Pitija, K., Sunpapao, A., 2022. A rhizobacterium, *Streptomyces albulus* Z1-04-02, displays antifungal activity against sclerotium rot in mungbean. Plants 11, 2607. https://doi.org/10.3390/plants11192607.

Saini, N., Bundela, V., Singh, S., Sahgal, M., Singh, A.V., 2024. Optimizing siderophore production in *Bacillus subtilis* to enhance seed germination and biocontrol efficacy against *Alternaria triticina* and *Bipolaris sorokiniana*. J. Sci. Res. Rep. 30, 313–326. https://doi.org/10.9734/jsrr/2024/v30i82251.

Seemann, T., 2014. Prokka: rapid prokaryotic genome annotation. Bioinformatics (Edam) 30, 2068–2069. https://doi.org/10.1093/bioinformatics/btu153.

Sharf, W., Javaid, A., Shoaib, A., Khan, I.H., 2021. Induction of resistance in chili against *Sclerotium rolfsii* by plant-growth-promoting rhizobacteria and *Anagallis arvensis*. Egypt. J. Biol. Pest Control 31, 16. https://doi.org/10.1186/s41938-021-00364-y.

Warmink, J.A., Nazir, R., Corten, B., van Elsas, J.D., 2011. Hitchhikers on the fungal highway: the helper effect for bacterial migration via fungal hyphae. Soil Biol. Biochem. 43, 760–765. https://doi.org/10.1016/j.soilbio.2010.12.009.

Wick, R.R., Judd, L.M., Gorrie, C.L., Holt, K.E., 2017. Unicycler: resolving bacterial genome assemblies from short and long sequencing reads. PLoS Comput. Biol. 13, e1005595. https://doi.org/10.1371/journal.pcbi.1005595.

Yang, C.R., Zhang, Y., Jacob, M.R., Khan, S.I., Zhang, Y.J., Li, X.C., 2006. Antifungal activity of C-27 steroidal saponins. Antimicrob. Agents Chemother. 50, 1710–1714. https://doi.org/10.1128/AAC.50.5.1710-1714.2006.

Zhang, N., Lv, F., Qiu, F., Han, D., Xu, Y., Liang, W., 2023. Pathogenic fungi neutralize plant-derived ROS via Srpk1 deacetylation. EMBO J. 42, e112634. https://doi.org/10.15252/embj.2022112634.

Zhang, Z., Chen, Y., Li, B., Chen, T., Tian, S., 2020. Reactive oxygen species: a generalist in regulating development and pathogenicity of phytopathogenic fungi. Comput. Struct. Biotechnol. J. 18, 3344–3349. https://doi.org/10.1016/j.csbj.2020.10.024.

Zhu, Q., Ma, Y., Zhang, T., Liu, W., Zhang, S., Chen, Y., Peng, D., Zhang, X., 2025. Biocontrol potential of rhizosphere bacteria against *Fusarium* root rot in cowpea: suppression of mycelial growth and conidial germination. Biol 14, 921. https://doi.org/10.3390/biology14050921.